*Organogenesis*, 12:128–142, 2016

ISSN: 1547-62781555-8592 online
DOI: 10.1080/15476278.2016.1185584

## *RESEARCH PAPERS*

# Decellularized spleen matrix for reengineering functional hepatic-like tissue based on bone marrow mesenchymal stem cells

Junxi Xiang,[a,b] Xinglong Zheng,[a,b] Peng Liu,[a,b] Lifei Yang,[b] Dinghui Dong,[a,b] Wanquan Wu,[a,b] Xuemin Liu,[a,b] Jianhui Li,[b,c] and Yi Lv[a,b]

[a]Department of Hepatobiliary Surgery, First Affiliated Hospital of Xi'an Jiaotong University, Xi'an, China
[b]Regenerative Medicine and Surgery Engineering Research Center of Shaanxi Province, Xi'an, China
[c]Department of Surgical Oncology, Shaanxi Provincial People's Hospital, Xi'an, China

**ABSTRACT.** *Background and Aims*: Decellularized liver matrix (DLM) hold great potential for reconstructing functional hepatic-like tissue (HLT) based on reseeding of hepatocytes or stem cells, but the shortage of liver donors is still an obstacle for potential application. Therefore, an appropriate alternative scaffold is needed to expand the donor pool. In this study, we explored the effectiveness of decellularized spleen matrix (DSM) for culturing of bone marrow mesenchymal stem cells (BMSCs), and promoting differentiation into hepatic-like cells.

*Methods*: Rats' spleen were harvested for DSM preparation by freezing/thawing and perfusion procedure. Then the mesenchymal stem cells derived from rat bone marrow were reseeded into DSM for dynamic culture and hepatic differentiation by a defined induction protocol.

*Results*: The research found that DSM preserved a 3-dimensional porous architecture, with native extracellular matrix and vascular network which was similar to DLM. The reseeded BMSCs in DSM differentiated into functional hepatocyte-like cells, evidenced by cytomorphology change, expression

Correspondence to: Yi Lv; Email: luyi169@126.com; Department of Hepatobiliary Surgery, First Affiliated Hospital of Xi'an Jiaotong University. No. 277 West Yanta Road, Xi'an, Shaanxi, 710061, P. R. China.
Received February 1, 2016; Revised April 16, 2016; Accepted April 29, 2016.
Color versions of one or more of the figures in the article can be found online at www.tandfonline.com/kogg.

of hepatic-associated genes and protein markers, glycogen storage, and indocyanine green uptake. The albumin production (2.74±0.42 *vs*. 2.07±0.28 pg/cell/day) and urea concentration (75.92±15.64 *vs*. 52.07±11.46 pg/cell/day) in DSM group were remarkably higher than tissue culture flasks (TCF) group over the same differentiation period, $P < 0.05$.

*Conclusion*: This present study demonstrated that DSM might have considerable potential in fabricating hepatic-like tissue, particularly because it can facilitate hepatic differentiation of BMSCs which exhibited higher level and more stable functions.

**KEYWORDS.** bone marrow mesenchymal stem cells, decellularized scaffold, differentiation, liver tissue engineering, spleen

## INTRODUCTION

Liver transplantation remains currently the only curative mode of management for end stage liver disease, but seriously limited by severe shortage of donor organs. This predicament have sparked tremendous interest in finding new treatments. One promising approach to address the issue of donor shortage is decellularized liver matrix (DLM)-based tissue engineering, specifically, reseeding hepatocytes in DLM to reconstruct hepatic-like tissue (HLT) for compensatory liver function.[1,2] Unlike previously used synthetic or natural 3-dimensional materials,[3-5] the decellularized scaffold offers a desirable environment for cell adhesion, proliferation, maturation and functioning[6,7] because it retains site-specific natural extracellular matrices (ECM) and basic organ skeletal structures, which are difficult to reproduce artificially. Moreover, the vascular networks preserved in the decellularized scaffold also provide channels for perfusion and implantation *in vivo*. Studies have demonstrated that decellularized matrix based tissue regeneration is feasible for many hollow and parenchyma organs, such as bladder,[8] skin,[9] blood vessels,[10] heart,[11] lung,[12] kidney,[13] as well as liver.[14]

Nonetheless, potential clinical application of DLM-based HLT may be plagued by the selection of scaffold source, considering that human derived DLM is also insufficient, and the application of xenogeneic DLM is hindered by potential risks of zoonosis and immunological rejection. Herein, in order to expand the scaffold donor pool, we have established the decellularized spleen matrix (DSM), which had homogeneous ECM with DLM, and presented comparable condition for hepatocyte cultivation.[15,16] DSM scaffolds may be more promising for clinical application due to their extensive sources such as traumatic rupture, hypersplenism caused by various reasons, idiopathic thrombocytopenic purpura, floating spleen, and donation after cardiac/brain death.

With a view toward clinical translation, we sought to engineer DSM-based HLT with bone marrow mesenchymal stem cells (BMSCs). This strategy possesses more significant potential for liver tissue engineering compared with hepatocytes or cells from embryos, because of its easy accessibility, rapid proliferation, multipotent differentiation, and immunological tolerance.[17-19] Several studies[20-23] have also showed that transplantation of BMSCs or BMSC-derived hepatocytes could improve the liver function in laboratory animals or patients suffering from liver damage.

In this present study, we improved the technique for preparing DSM scaffold, and demonstrated that the DSM can provide a microenvironment mimicking DLM and also promotes the hepatic differentiation of BMSCs into high yields of functional hepatocyte-like cells. This work in this study indicates that DSM is a promising scaffold for BMSCs-based HLT.

## RESULTS

### Characteristics of DSM scaffold

During the decellularization process, a translucent DSM scaffold which retained the gross shape

of spleen was generated gradually (Fig. 1b). H-E staining showed the presence of eosinophilic staining that is typical of collagen, but no basophilic cellular nuclear staining was detected (Fig. 1c). A lack of DAPI staining in the DSM confirmed the absence of nuclear material (Fig. 1d). DNA content of the DSM was 25.03± 4.68 ng/mg dry weight, which represents 0.49% of the total content of native spleen (5040± 675.1 ng/mg dry weight, $P < 0.05$), and electrophoretic analysis confirmed that the residual DNA material consisted of fragments <200 bp in

FIGURE 1. Decellularization and characterization of rat decellularized spleen. (a) Schematic representation of the sequential whole-spleen decellularization protocol. (b) General appearance of rat spleen at various steps in the decellularization process. H-E (c), DAPI (d) staining and remnant DNA analysis (e, f) confirmed the degradation of cell contents. (g) SEM images showing the absence of cellular material but preservation of 3-dimensional porous architecture. (h) Immunofluorescent staining with similar ECM components of DSM as native spleen. Scale bars: 50 $\mu$m (c), (d), (h), 20 $\mu$m (g).

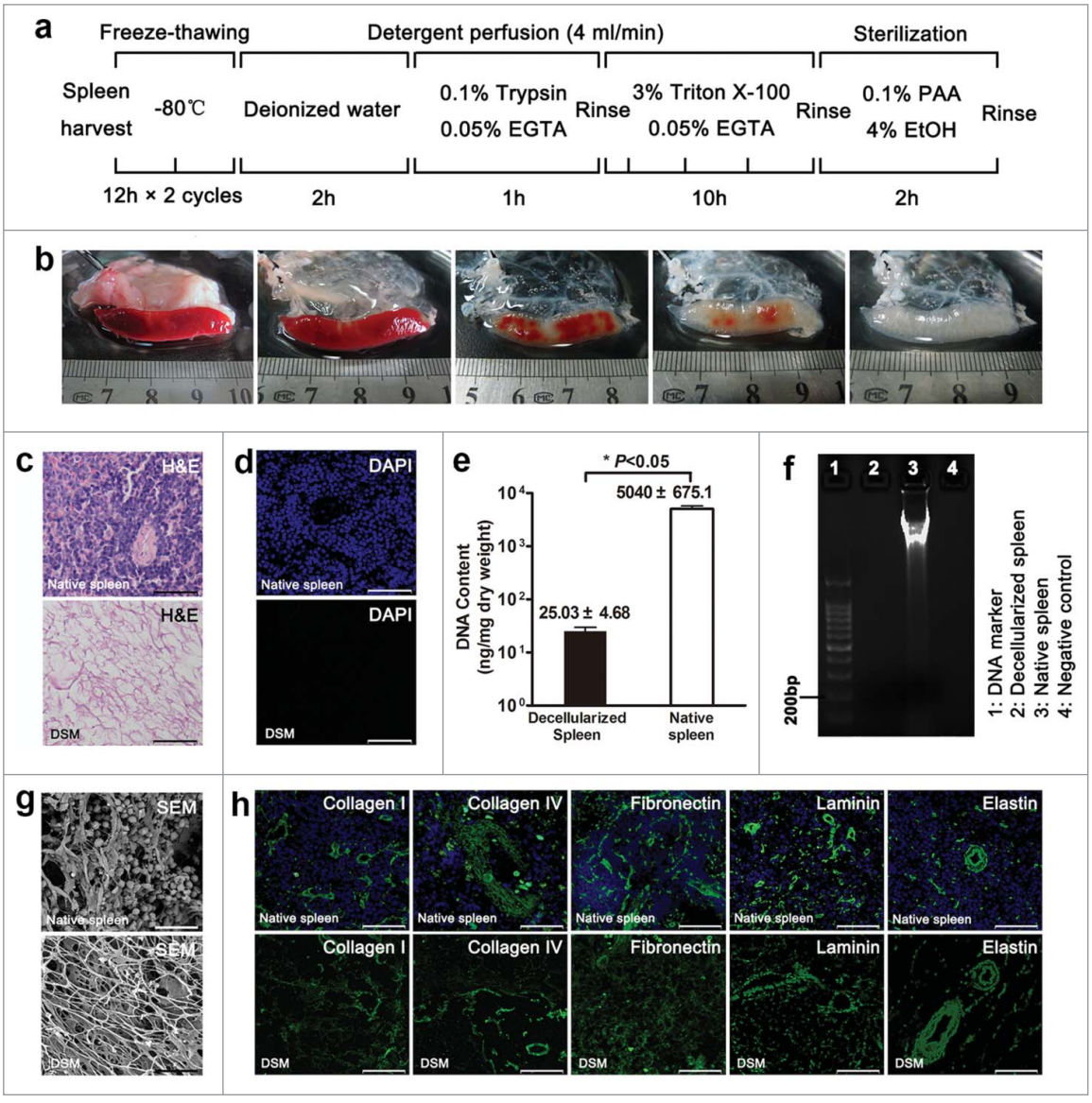

length, confirming that degradation of cell contents was extensive (Fig. 1e and 1f). The residual DNA and DAPI staining reached the acceptable standards for decellularization.[1,2] Scanning electron microscopy (SEM) images confirmed the presence of collagen fibers within the DSM (Fig. 1g). We also observed voids of 20 $\mu$m in diameter, resembling the honey-comb structure, which could be the footprint of cells removal by decellularization. The preservation of crucial ECM proteins, including collagen I, collagen IV, fibronectin, laminin and elastin in the DSM, was verified by positive immunostaining of these ECM components (Fig. 1h), indicating a similar structural composition of the matrix to that of native spleen and liver.

### *Characterization and differentiation potential of BMSCs*

The BMSCs expanded easily in culture and presented a fibroblast-like morphology through serial passages with a uniform pattern (Fig. 2a). There were no notable differences between passage 3, 5 and 8 groups except that the growth curve of passage 8 cells was slightly lower (Fig. 2b). Flow cytometry analysis revealed that most cells expressed the standard BMSCs surface markers CD29 (96.6±2.8%), CD44 (84.3±11.1%) and CD90 (88.9±8.4%), whereas negative for CD34 (1.5±1.3%) and CD45 (6.1±2.8%) (Fig. 2c). Two weeks after exposure to adipogenic and 4 weeks after osteogenic and chondrogenic differentiation medium, we observed intracellular lipid droplets, extracellular calcium phosphate precipitates, and chondrocytes using Oil Red O, Alizarin-Red and Toluidine-Blue staining (Fig. 2d), respectively. These results suggested that the BMSCs were generated successfully and could be used in the following experiments.

### *Establishing of HLT and cytomorphology observation*

About $2 \times 10^7$ BMSCs were infused into the DSM and the engraftment efficiency with the multistep infusion protocol was 88.1%±2.4%. A representative image of the construct before and after recellularization process was shown in Fig. 3a. During hepatic differentiation in TCF culture, the morphology of the BMSCs evolved from spindle to cuboidal shape gradually. Cell viability was maintained during the dynamic culture and distributed in the DSM parenchyma sites through network of blood vessels. H-E staining presented cells with round nucleus, prominent nucleoli, and polygonal cytoplasm on day 21, which were similar with typical morphology of hepatocytes (Fig. 3c). The TUNEL-positive cell percentage was (14.1 ± 3.7) % at the end of dynamic culture.

To confirm the ultrastructure characteristics, undifferentiated and differentiated BMSCs cultured in the DSM scaffold were examined using electron microscope on day 0 and 21. The BMSCs on day 0 (Fig. 3d i,iii,v) exhibited a spindle morphology with few surface microvilli and contained a high nuclear/cytoplasm ratio with very few immature cytoplasmic structures. The hepatocyte-like cells on day 21 exhibited a polygonal morphology with more and larger microvilli, a significantly reduced nuclear/cytoplasm ratio and an abundance of cytoplasmic structures (Fig. 3d ii,iv). The TEM micrograph of a portion of a single hepatocyte-like cell revealed an abundance of rough and smooth endoplasmic reticulum, mitochondria, Golgi apparatus, and glycogensome in the cytoplasm (Fig. 3d vi,vii,viii). These electron microscope images suggest that during the differentiation period, the ultrastructure of cells cultured in the DSM scaffold was transformed from those characteristics of stem cells to those of mature hepatocytes.

### *Gene expression and protein markers of BMSCs-derived hepatocytes*

A comparison of gene expression during hepatic differentiation of BMSCs within the DSM and TCF culture were carried out by RT-PCR (Fig. 4). The mRNA expression of the octamer-binding transcription factor 4 (OCT4) of BMSCs cultured in TCF decreased slowly over 21 days, whereas a significant reduction of OCT4 expression was detected

FIGURE 2. The characterization of BMSCs. Morphological identification (a) and proliferative activity (b) of BMSCs in passage 3, 5 and 8. (c) Surface antigen assay of BMSCs by flow cytometry indicated positive CD29, CD44, CD90 and negative CD34 and CD45. (d) Multipotency determination of BMSCs by adipogenic, osteogenic and chondrogenic induction. Scale bars: 30 $\mu$m.

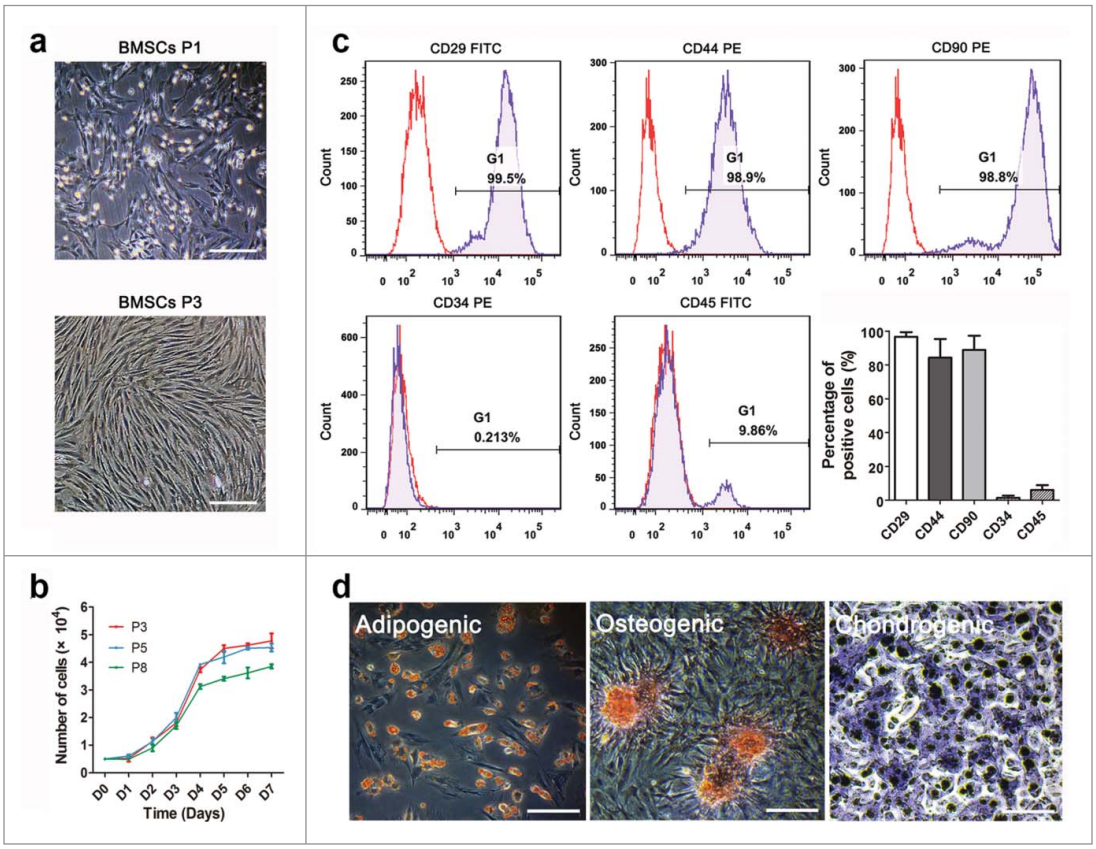


in HLT, suggesting the loss of pluripotency during the differentiation. The mRNA expression levels of liver generated plasma proteins ALB and AFP in HLT increased significantly in a time-dependent manner and on day 21, were significantly higher compared to those in TCF-cultured cells. In addition, the transcription levels of various hepatic development associated genes, such as hepatocyte nuclear factor 1 $\alpha$ (HNF1A), nuclear factor 4 $\alpha$ (HNF4A), forkhead box A2 (FOXA2) and cytokeratin-18 (CK18) exhibited a significant increase in HLT than in TCF culture. In the DSM scaffold the mRNA expression of hepatic functional associated genes and hepatic metabolic enzymes, namely transthyretin (TTR), a-1-antitrypsin (A1AT), glucose-6-phosphatase, catalytic (G6PC), and members of the cytochrome P450 subunits CYP1A2, was detected earlier and higher than those in the TCF group.

We further analyzed the expression of CD90, protein marker of undifferentiated BMSCs, and various hepatic progenitor markers, namely AFP, ALB, CK8 and CK18 using immunofluorescence staining (Fig. 5) at the end of differentiation stage, to confirm the *in vitro* hepatic differentiation. A portion of the cells in TCF presented weak fluorescence signal of CD90, as well as hepatic progenitor markers staining, even if supplementing with growth factors. However, higher AFP, ALB, CK8 and CK18 expression observed from the cells in HLT may represent the phenotype of hepatic progenitors, whereas CD90 positive cells were not detected.

FIGURE 3. Scaffold recellularization and hepatic differentiation of BMSCs. (a) The representative photographs of DSM before and after repopulation and the dynamic culture system. (b) Schematic representation of the hepatic differentiation protocol. (c) Cytomorphology and reengineered hepatic-like tissue (HLT) observed by phase-contrast microscope and H-E staining. (d) Ultrastructural characters of undifferentiated BMSCs (i, iii, v) and hepatocyte-like cells (ii, iv, vi-viii) in DSM culture. Scale bars: 30 $\mu$m (c), 1 $\mu$m ((d) i-iv), 300 nm ((d) v-viii).

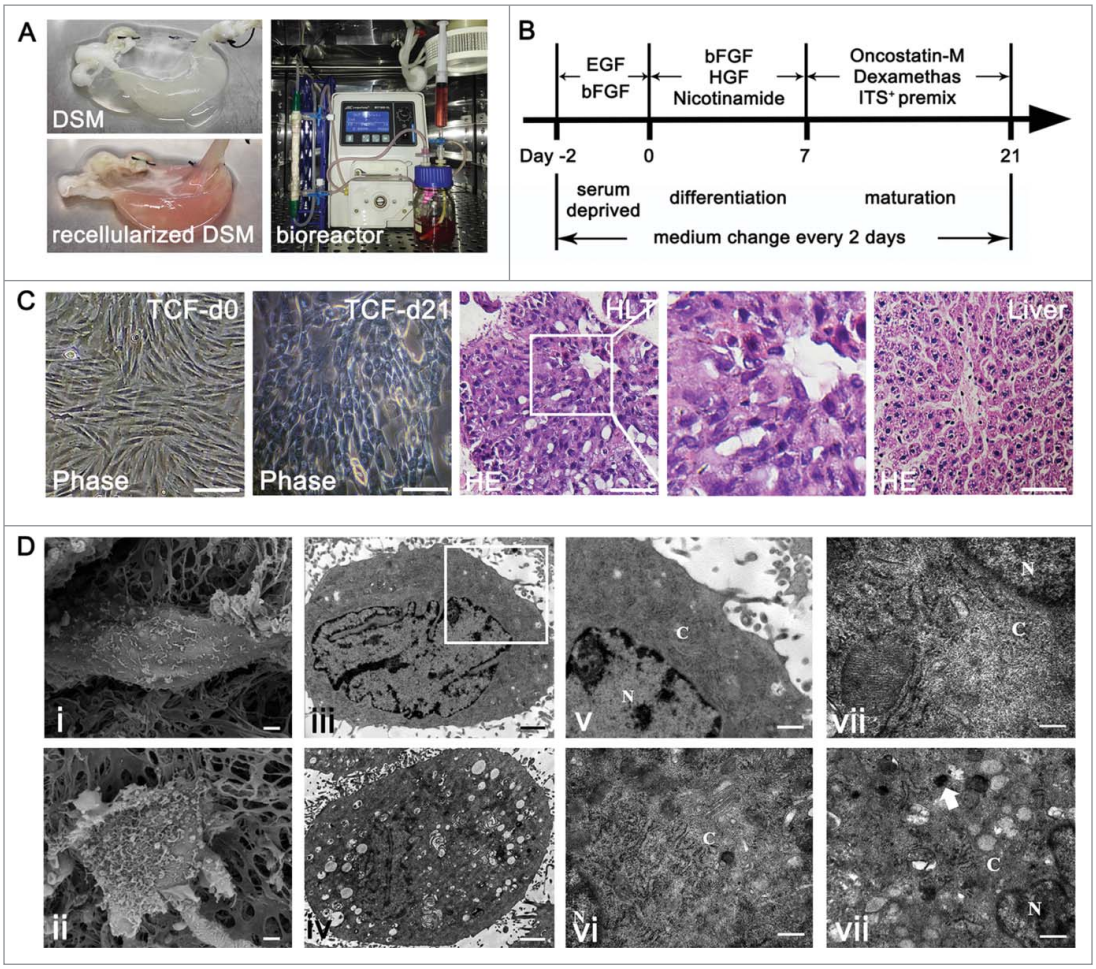


## *In vitro functional analysis of differentiated BMSCs in HLT and TCF*

The PAS staining demonstrated that a portion of positive cells exhibited a red-purple cytoplasm when cultured in hepatic inducing medium as previously described, indicating the glycogen storage (Fig. 6a). The positive rate of PAS staining in TCF group was (39.4±4.2)%, less than the rate of (51.5±6.3)% in HLT group. In addition, we used the uptake of ICG assay to determine the hepatic metabolic functions and to identify BMSCs derived hepatocytes *in vitro*. The result revealed that the positive staining rate in TCF group was (33.1±1.1)%, significantly lower than that of (53.0±3.0)% in HLT group and (61.6±2.1%) in fresh liver (Fig. 6b).

In order to further evaluate the metabolic activity, albumin secretion and urea production by the BMSCs derived hepatocytes in HLT and TCF culture were quantified at different time points during hepatic differentiation (Fig. 6c). The production of ALB by the HLT group was significantly higher than the TCF group on day 14 (2.44±0.17 *vs.* 1.64±0.36 pg/cell/day, $P =$

FIGURE 4. RT-PCR analysis of liver-specific genes expression by BMSCs-derived cells cultured in tissue culture flasks (TCF) and DSM. The undifferentiated BMSCs and primary hepatocytes were used as controls.

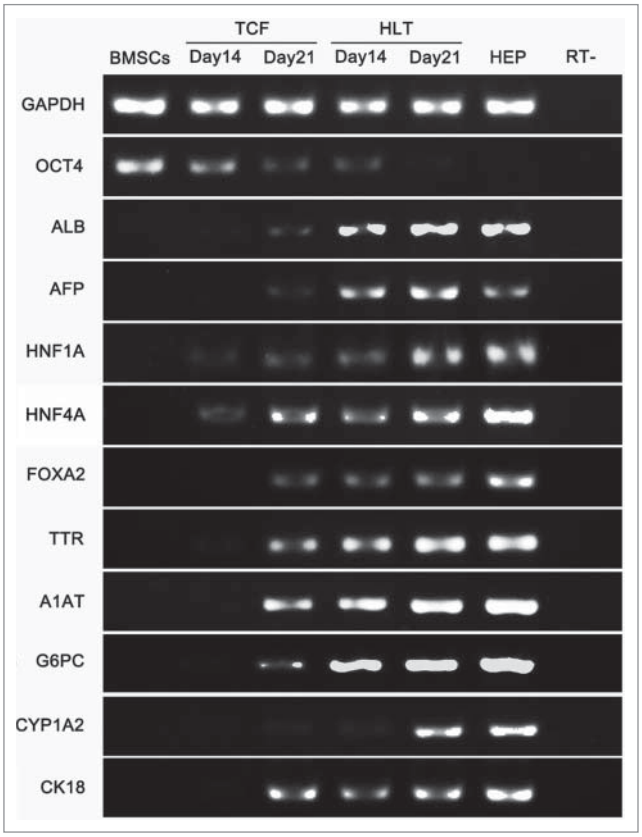


0.001) and on 21 d (2.74±0.42 *vs*. 2.07±0.28 pg/cell/day, $P = 0.009$). The urea concentration of the HLT culture medium was remarkably higher that of the TCF culture medium on 14 d (51.58±10.28 *vs*. 30.07±6.56 pg/cell/day, $P = 0.002$) and on day 21 (75.92±15.64 *vs*. 52.07± 11.46 pg/cell/day, $P = 0.013$) over the same differentiation period. The results clearly demonstrate the superiority of the DSM dynamic culture over TCF culture in terms of supporting metabolic function expression of hepatocyte-like cells.

## *Discussion*

The scaffold materials, seed cells and environment signals for organizational integration and tissue cultivation are the 3 key elements of tissue engineering.[24,25] In this present study, a natural extracellular matrix scaffold from the decellularized spleen was used to optimize the differentiation of BMSCs toward higher functional hepatocytes and improved regeneration of hepatic-like tissue. The results demonstrated that the 3-dimensional DSM scaffold with favorable biocompatibility was suitable for cell engraftment, and facilitated significantly better lineage-specific differentiation in combination with growth factors *in vitro*, compared to the 2-dimensional TCF culture system.

The feasibility of liver reconstruction based on DLM and hepatocytes or stem cells [26-29] has been demonstrated in rodent, goat and swine, which has stimulated a decellularization upsurge worldwide. The ultimate goal of decellularization is to apply engineered HLT in clinical work. However, the limited source of human DLM-based hepatic-like tissue further urges research in reconstructing DSM-based

FIGURE 5. Protein markers expression of BMSCs-derived cells in TCF and HLT analyzed using immunofluorescence staining at the end of differentiation stage. The undifferentiated BMSCs and fresh livers were used as controls. Scale bars: 20 $\mu$m.

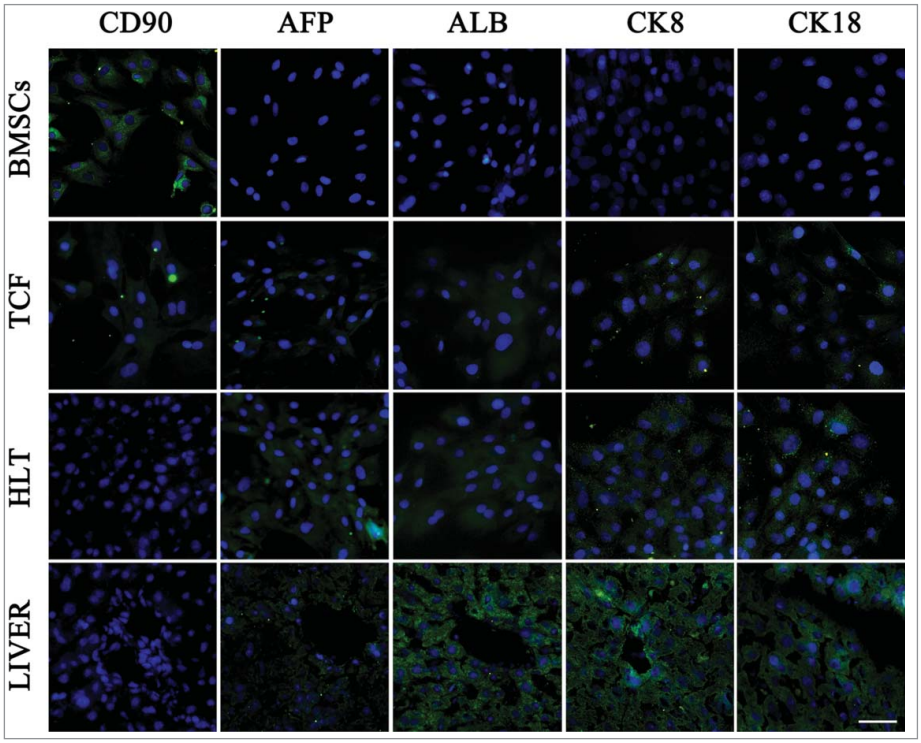


HLT for future clinical applications. Using DSM for liver reconstruction is not to replace DLM, but to expand the scaffold donor pool. Even though DLM is the optimal choice, DSM may be an option which could relieve the donor shortage. DSM could derived from removed spleen such as traumatic rupture, hypersplenism caused by various reasons, idiopathic thrombocytopenic purpura, floating spleen, and donation after cardiac/brain death. Take organ donation for example, more than 2500 cases of donation after cardiac death were performed in 2015 in China and the data was still increasing. Compared with animal organs, human derived DSM is an alternative with closer homology of proteins and lower potential risk of zoonosis infection. This strategy may have the potential of significantly expanding the donor pool provided that hepatic-like tissue can be reconstructed successfully.

In this study, we adopt an improved sequential approach to reduce the ECM damage and spleen decellularization duration. The procedure of repeating freezing and thawing and hypotonic deionized water perfusion could physically disrupt cell membranes to facilitate the decellularization process while avoiding disruptions of ECM. Although deionized water could solubilize collagen types and forms, the reduction of collagen in limited time was acceptable according to morphological observation and collagen quantification. More importantly, the use of deionized water reduced the dosage and duration of detergents which were even more damage to ECM and reseeded cells. Triton X-100, a relatively milder nonionic detergent than sodium dodecyl sulfonate, was used to achieve better extracellular matrix retention.[30] The DSM produced by this strategy presented similar porous architecture and native ECM component compared with DLM according to our data and previous research.[2,31-33] Another study by our team measured the collagen and sGAG contents and

FIGURE 6. Functional analysis of differentiated cells in TCF and HLT. (a) Glycogen storage assessed by Periodic acid-Schiff assay on BMSC-derived hepatocyte-like cells in TCF and HLT. (b) The metabolic potential of the BMSCs-derived cells was determined by uptake of indocyanine green at the end of differentiation. The undifferentiated MSCs and fresh liver were used as controls. (c) Albumin secretion and urea production by the BMSCs-derived cells were analyzed at various development stages using the TCF and HLT approaches (*P $<$0.05, **P$<$0.01). Scale bars: 30 $\mu$m.

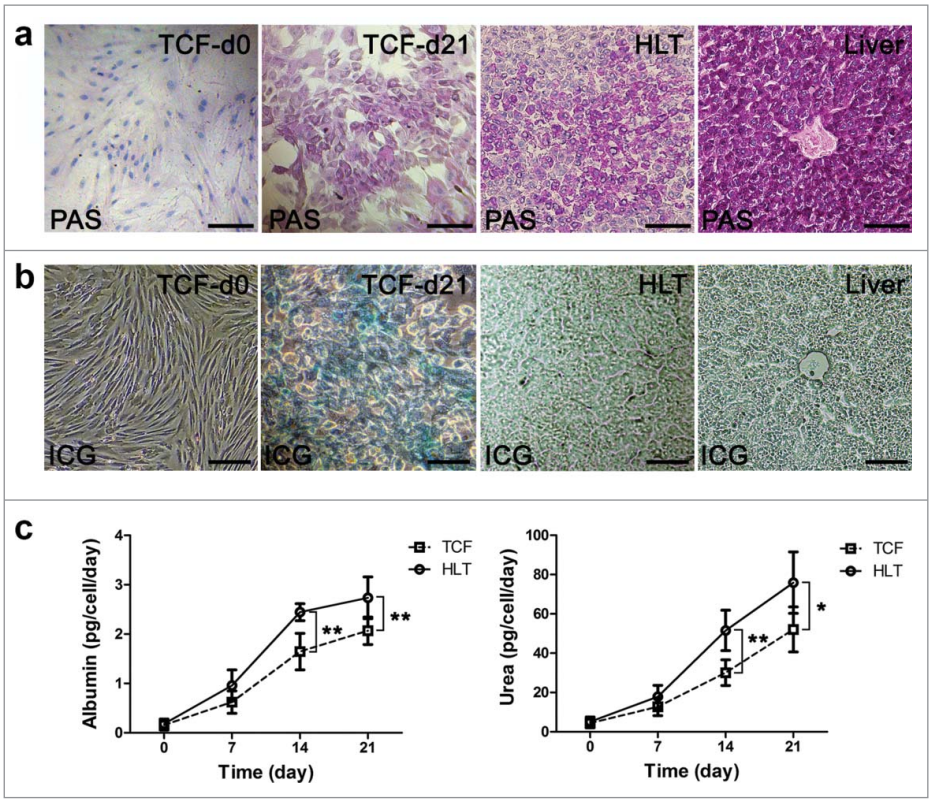


compared them between DSM and DLM. The result revealed that there were not significant differences (data not shown). Remarkably, an abundant blood sinus structure was observed in DSM, which was favorable to satisfy the large amount of cell metabolism and oxygen consumption. It has been concluded in our published reports[15,16] that the hepatocyte vitality when cultured in DSM as well as the synthesis and secretion function were comparable with DLM-based HLT.

In consideration of the shortage of hepatocytes from donor livers, we used BMSCs which possess the potential to differentiate into functional hepatocyte-like cells. Besides, the use of BMSCs can also bypass the ethical controversies. Ji[34] and Jiang[35] *et al*. have shown that DLM can effectively promote hepatic differentiation of BMSCs *in vitro* by a defined protocol. To investigate the effect of DSM on BMSCs under hepatic differentiation, we have cultured BMSCs in DSM or TCF with the same induction medium and further validated the cell morphology and function. The electron microscope images presented abundant metabolic organelles after differentiation. In addition, we observed up-regulations of liver-specific transcription factors, biotransformation enzymes and hepatic-lineage plasma proteins in BMSCs cultured in DSM and the expression level was significantly higher than that in TCF culture, but the BMSCs cultured in DSM gradually lost their multipotency. Meanwhile, more cells in DSM culture expressed higher levels of hepatic

markers by immunofluorescence, but CD90 positive cells were not detected on the contrary, suggesting that the DSM scaffold presented the independent inductive potential for the differentiation of BMSCs into the hepatic lineage. The analysis of metabolic functions demonstrated that the hepatocyte-like cells in DSM scaffold exhibited more abundant and stable function than those in TCF culture, including glycogen storage and ICG uptake, which were consistent with the gradually increasing albumin synthesis and urea secretion.

Nonetheless, the maturation degree of hepatocyte-like cells derived from BMSCs still fell insufficient of mature hepatocytes, not only for gene expression but also for metabolic function. This phenomenon may be related to the differences between *in vitro* and more complex microenvironment *in vivo*. Implanting the graft *in vivo* may be the optimum solution to relieve this awkward situation, as the body will allow the cells to obtain enough oxygen and nutrition, suitable growth factors and intercellular interaction as in normal physiological conditions.[36]

Although this is the first attempt to induce hepatic differentiation of BMSCs in the DSM scaffold, there are still some limitations and questions remained unclear. First of all, further research is required to investigate the possible pathological changes of DSM derived from diseased spleen and the feasibility of cell reseeding. In addition, the effect of DSM and DLM cultures on the differentiation and proliferation efficiency of BMSCs should be compared. Most importantly, *in vivo* implantation of the DSM-based HLT is worthy of being explored as an organized and functional liver-tissue equivalents for acute or chronic hepatic injuries. Even if the regeneration of an entire liver will be a promising but challenging task, a piece of HLT with part of the hepatic function is needed for many patients rather than an entire liver.[37] Therefore, it is feasible for some clinical cases to replace part of the liver function by implanting recellularized HLT based on DSM.

In summary, we successfully developed a strategy for the production of DSM in which the inherent ultrastructure and native ECM were preserved. The DSM bio-scaffold might have considerable potential for cell-based therapy and liver tissue engineering research, particularly because it promotes the differentiation of BMSCs into hepatocyte-like cells by a defined protocol, which exhibited higher level and more stable functions. Further investigation of HLT implantation is necessary to realize the functional expression *in vivo* and to promote the translation into clinical application.

## MATERIALS AND METHODS

### Spleen harvest and whole-organ decellularization

The whole spleens were harvested from healthy Sprague-Dawley rats weighing 200∼250 g. All protocols were approved by the Institutional Animal Care and Use Committee of Xi'an Jiaotong University. The rats were anesthetized by sodium pentobarbital and systemic heparinized with 1000 U intraperitoneal injection, followed by a cross-abdominal incision. An intravenous catheter (24 G) was inserted into splenic artery and heparinized PBS (100 U/mL) was infused by peristaltic pump at a speed of 4 mL/min for 30 min. Then the spleen was isolated with intact splenic vessels and perfused with deionized $H_2O$ for one hour. Subsequently, the sample was processed by 12 h freezing/thawing $\times 2$ cycles at $-80°C$ to aid in cell lysis.

Decellularization procedure was conducted by a peristaltic pump at 4 mL/min through the cannula into splenic artery, and the perfusion process was carried out as follows (Fig. 1a). Deionized water perfusion for 2 h following 0.1% trypsin (Amresco)/ 0.05% EGTA (MP Biomedicals) solution at 37°C for 1 h. After rinsing with deionized water for 30 min, the 3% Triton X-100 (MP Biomedicals)/ 0.05% EGTA solution was perfused for 10 h and the solution was changed after 1, 4 and7 hours. A deionized water rinsing for 30 min was conducted followed by sterilizing with 0.1% (v/v) peracetic acid (PAA) / 4% EtOH perfusion for 2 h, and then neutralized by sterile PBS for 30 min twice.

### *Isolation and cultivation of BMSCs*

BMSCs were harvested by flushing the bone marrow of femurs and tibias of 6∼10 week male Sprague–Dawley rats, using Dulbecco's Modified Eagle Medium/ Nutrient Mixture F12 (DMEM/ F12) Medium (HyClone) containing 10% fetal bovine serum (FBS, Gibco). Following filtration through a 200 mesh screen and centrifugation at 800 rpm for 5 min, the resuspended single-cell was cultured in 10 $cm^2$ tissue culture flasks (TCF) at 37°C / 5% $CO_2$ incubator. The non-adherent cells were removed after 24 h by rinsing and replacing the medium. At about 70% confluence, the cells were passaged at a ratio of 1:2. The third passage cells were characterized by surface antigen CD29, CD44, CD90, CD34 and CD45 using flowcytometry; the differentiation potential along the adipogenic, osteogenic and chondrogenic lineages was verified as previously described.[38]

### *Recellularization of DSM scaffold and dynamic culture*

The DSM scaffolds had culture medium perfusion for 1 h prior to recellularization. BMSCs at passage 3∼8 were resuspended to $5 \times 10^6$/ mL and a total of $2 \times 10^7$ cells were introduced into each DSM scaffold at a speed of 1 mL/ min. BMSCs were infused into DSM using 4 steps at 15 min intervals. After 2 h stationary culture in DMEM/F12 medium containing 10% FBS to allow cell adherence, the perfusate was collected to determine the cell viability and the retention rate in the scaffold. Subsequently, the recellularized DSM was connected into the dynamic culture system consisted of a clean chamber containing 60 ml perfusate, peristaltic pump, bubble trap and oxygenator which connected to a gas mixture of 95% $O_2$ and 5% $CO_2$ and placed in a standard 37°C incubator (Fig. 3a). The medium was perfused at a flow rate of 1 mL/min and was replaced every other day.

### *In vitro hepatic differentiation of BMSCs*

Hepatic differentiation was induced by treating the BMSCs in DSM scaffold or in TCF for comparison for 4 weeks with a 2-step protocol with minor modifications (Fig. 3b). In brief, the stem cells were serum deprived for 2 days, in Iscove's modified Dulbecco's Medium (IMDM, HyClone) supplemented with 20 ng/ mL epidermal growth factor (EGF, Invitrogen) and 10 ng/mL basic fibroblast growth factor (bFGF, Invitrogen).Thereafter, differentiation was induced by treating BMSCs with step-1 differentiation medium, consisting of IMDM supplemented with 10 ng/mL bFGF, 20 ng/mL hepatocyte growth factor (HGF, R&D) and 0.61 mg/mL nicotinamide (Sigma) for 7 days, followed by step-2 maturation medium treatment, consisting of IMDM supplemented with 20 ng/mL oncostatin M (Sigma), 1 $\mu$mol/L dexamethasone(Sigma), and 50 $\mu$g/mL $ITS^+$ premix (Sigma) for 14 d. Medium replacement was performed every 2 d.

### *Morphologic and histological evaluation*

Tissue samples were fixed in 10% neutral buffered formalin, embedded in paraffin, and sectioned into 4 $\mu$m section for hematoxylin and eosin (H-E) or periodic acid-schiff (PAS, JIANCHENG Biotech) staining according to the manufacturer's recommendation. For immunofluorescence analysis, tissue samples were cryostat sectioned followed by permeabilization, blocking using 5% bovine serum albumin (BSA, Sigma) and incubating over night at 4°C with the primary monoclonal antibodies including collagen I, collagen IV, fibronectin, laminin, elastin, CK18 (1:400, Abcam), CD90, AFP (1:100, Bioworld), ALBand CK8 (1:200, Santa). Thereafter, the samples were incubated with secondary antibody at 37°C for 1 h and counterstained using 4′,6-diamidino-2-phenylindole (DAPI, Sigma). Optical images were taken using Olympus BX53F microscope.

For scanning electron microscopy (SEM) analysis, specimens were fixed with 2.5% glutaraldehyde for 2 h and post-fixed with 1% osmium tetroxide for 1 h, following dehydrating by graded series of ethanol for 15 min each (30%, 50%, 70%, 90%, 100%). After dried at critical point for 2 h and sputter-coated with gold-palladium, samples were visualized using a Hitachi TM-1000

SEM system. For transmission electron microscopy (TEM), the cell clumps were post-fixed using osmium tetroxide, and were cut into ultrathin sections prior to loading into a Hitachi H-7500 TEM system.

### *DNA content analysis*

DNA extraction was performed using Genomic DNA Kit (TIANGEN Biotech) according to the manufacturer's instructions. The total amount of DNA was quantified using the ultramicro ultraviolet spectrophotometer (Quawell). Remnants base pair analysis of the sample was performed by gel electrophoresis.

### *RNA extraction and RT-PCR analysis*

At different stages during differentiation in DSM or TCF, total RNA was isolated by using Trizol Reagent (Sigma) following the manufacturer's instruction. The sample absorbance at 280 nm and 260 nm was measured using a Varioskan Flash (Thermo) to obtain the concentration and quality of RNA. Reverse transcription was performed using a PrimeScript RTkit (Takara) following polymerase chain reaction (PCR) amplification using the rat-specific primers (DINGGUO Biotech) listed in Table 1. The products were analyzed by gel electrophoresis and were visualized on a gel imaging and analysis system (BIORAD). The undifferentiated BMSCs and fresh primary hepatocytes were used as the negative and positive controls.

### *Indocyanine green (ICG) uptake analysis*

For ICG uptake analysis, cardiogreen (Sigma) was diluted in serum-free IMDM medium to a final concentration of 1 mg/mL. Afterwards, the diluted ICG solution was added to the cell culture dishes or perfused into HLT for incubating at 37°C for 30 min. Finally, the cells and tissue were washed by PBS and were examined under microscope. Image J software was used to measure the optical density of positive staining for semi-quantitative analysis.

TABLE 1. Sequence of the primers and length of the products.

| Gene | Sequence of primers | Length (bp) |
|---|---|---|
| GAPDH | F: 5′ TGGAGTCTACTGGCGTCTT 3′<br>R: 5′ TGTCATATTTCTCGTCCTTCA 3′ | 138 |
| OCT4 | F: 5′ AAGTTGGCGTGGAGACTCTG 3′<br>R: 5′ GGACTCCTCGGGACTAGGTT 3′ | 143 |
| ALB | F: 5′ GTGAGCGAGAAGGTCACCAA 3′<br>R: 5′ TTTCACCAGCTCAGCGAGAG 3′ | 198 |
| AFP | F: 5′ CACCATCGAGCTCGGCTATT 3′<br>R: 5′ GAGACAGGAAGGTTGGGGTG 3′ | 186 |
| HNF1A | F: 5′ TGACTAGTGGGATTTGGGGGA 3′<br>R: 5′ TGCAGCTGGCTCAACTTAGA 3′ | 161 |
| HNF4A | F: 5′ ACCTCAACTCATCCAACAG 3′<br>R: 5′ GACACTGGTTCCTCTTATCT 3′ | 198 |
| FOXA2 | F: 5′ CCTACTCGTACATCTCGCTCATCA 3′<br>R: 5′ CGCTCAGCGTCAGCATCTT 3′ | 173 |
| TTR | F: 5′ CAGCAGTGGTGCTGTAGGAGTA 3′<br>R: 5′ GGGTAGAACTGGACACCAAATC 3′ | 120 |
| A1AT | F: 5′ CTTGGGAGCCAAGAACCTGAT 3′<br>R: 5′ TGGTCCTGCTGGGAGGTATC 3′ | 212 |
| G6PC | F: 5′ GGACCTCCTGTGGACTTTGG 3′<br>R: 5′ AAACGGAATGGGAGCGACTT 3′ | 192 |
| CYP1A2 | F: 5′ TCGGTGGCTAATGTCATCGG 3′<br>R: 5′ ACCGGAAAGAAGTCCACAGC 3′ | 140 |
| CK18 | F: 5′ GCCCTGGACTCCAGCAACT 3′<br>R: 5′ ACTTTGCCATCCACGACCTT 3′ | 197 |

### *Albumin and urea production*

The supernatants of the conditioned media from the differentiated BMSCs cultured in TCF and DSM were collected at days 0, 7, 14 and 21. The conditioned media were assayed for rat albumin and urea production using a chemistry analyzer (H-7650, HITACHI) following the manufacturer's instructions.

### *Statistical analysis*

All data are expressed as mean ±standard deviation and statistical analysis was carried out using SPSS software version 18.0.Analysis of variance followed a Student's *t* test was used to determine difference between the control and experimental group and $P$-value $< 0.05$ was considered to be statistically significant.

## *DISCLOSURE OF POTENTIAL CONFLICTS OF INTEREST*

No potential conflicts of interest were disclosed.

## *FUNDING*

This work was supported by grants from National Natural Science Foundation of China (81501608) and the Science and Technology Research and Development Program of Shaanxi Province (2012KW-39-01).

## REFERENCES

[1] Uygun BE, Soto-Gutierrez A, Yagi H, Izamis M-L, Guzzardi Ma, Shulman C, Milwid J, Kobayashi N, Tilles A, Berthiaume F, et al. Organ reengineering through development of a transplantable recellularized liver graft using decellularized liver matrix. Nat Med 2010; 16:814-20; PMID:20543851; http://dx.doi.org/10.1038/nm.2170

[2] Soto-Gutierrez A, Zhang L, Medberry C, Fukumitsu K, Faulk D, Jiang H, Reing J, Gramignoli R, Komori J, Ross M, et al. A whole-organ regenerative medicine approach for liver replacement. Tissue Eng Part C Methods 2011; 17:677-86; PMID:21375407; http://dx.doi.org/10.1089/ten.tec.2010.0698

[3] Chen AA, Thomas DK, Ong LL, Schwartz RE, Golub TR, Bhatia SN. Humanized mice with ectopic artificial liver tissues. Proc Natl Acad Sci U S A 2011; 108:11842-7; PMID:21746904; http://dx.doi.org/10.1073/pnas.1101791108

[4] Lee SA, No da Y, Kang E, Ju J, Kim DS, Lee SH. Spheroid-based three-dimensional liver-on-a-chip to investigate hepatocyte-hepatic stellate cell interactions and flow effects. Lab Chip 2013; 13:3529-37; PMID: 23657720; http://dx.doi.org/10.1039/c3lc50197c

[5] Duncan AW, Soto-Gutierrez A. Liver repopulation and regeneration: new approaches to old questions. Curr Opin Organ Transplant 2013; 18:197-202; PMID:23425785; http://dx.doi.org/10.1097/MOT.0b013e32835f07e2

[6] Rosado AM, Brewster LP. Regeneration: letting the scaffold do the work. J Surg Res 2013; 180:49-50; PMID:22316671; http://dx.doi.org/10.1016/j.jss.2011.11.1026

[7] Wang X, Cui J, Zhang BQ, Zhang H, Bi Y, Kang Q, Wang N, Bie P, Yang Z, Wang H, et al. Decellularized liver scaffolds effectively support the proliferation and differentiation of mouse fetal hepatic progenitors. J Biomed Mater Res A 2013; 102 (4):1017-25; PMID:23625886

[8] Atala A, Bauer SB, Soker S, Yoo JJ, Retik AB. Tissue-engineered autologous bladders for patients needing cystoplasty. Lancet 2006; 367:1241-6; PMID:16631879; http://dx.doi.org/10.1016/S0140-6736(06)68438-9

[9] Nam K, Matsushima R, Kimura T, Fujisato T, Kishida A. In vivo characterization of a decellularized dermis-polymer complex for use in percutaneous devices. Artif Organs 2014; 38:1060-5; PMID:24962020; http://dx.doi.org/10.1111/aor.12330

[10] L'Heureux N, McAllister TN, de la Fuente LM. Tissue-engineered blood vessel for adult arterial revascularization. N Engl J Med 2007; 357:1451-3; PMID:17914054; http://dx.doi.org/10.1056/NEJMc071536

[11] Ott HC, Matthiesen TS, Goh S-K, Black LD, Kren SM, Netoff TI, Taylor DA. Perfusion-decellularized matrix: using nature's platform to engineer a bioartificial heart. Nat Med 2008; 14:213-21; PMID:18193059; http://dx.doi.org/10.1038/nm1684

[12] O'Neill JD, Anfang R, Anandappa A, Costa J, Javidfar J, Wobma HM, Singh G, Freytes DO, Bacchetta MD, Sonett JR, et al. Decellularization of human and porcine lung tissues for pulmonary tissue engineering. Ann Thorac Surg 2013; 96:1046-55; discussion 55-6; PMID:23870827; http://dx.doi.org/10.1016/j.athoracsur.2013.04.022

[13] Song JJ, Guyette JP, Gilpin SE, Gonzalez G, Vacanti JP, Ott HC. Regeneration and experimental orthotopic transplantation of a bioengineered kidney. Nat Med 2013; 19(5):646-51

[14] Sabetkish S, Kajbafzadeh AM, Sabetkish N, Khorramirouz R, Akbarzadeh A, Ladi Seyedian SS, Pasalar P, Orangian S, Beigi RS, Aryan Z, et al. Whole-Organ Tissue Engineering: Decellularization and Recellularization of Three-Dimensional Matrix Liver Scaffolds. J Biomed Mater Res A 2014; 103 (4):1498-508; PMID:25045886

[15] Gao R, Wu W, Xiang J, Lv Y, Zheng X, Chen Q, Wang H, Wang B, Liu Z, Ma F. Hepatocyte Culture in Autologous Decellularized Spleen Matrix. Organogenesis 2015; 11(1):16-29:0

[16] Zheng X-L, Xiang J-X, Wu W-Q, Wang B, Liu W-Y, Gao R, Dong D-H, Lv Y. Using a decellularized splenic matrix as a 3D scaffold for hepatocyte cultivationin vitro: a preliminary trial. Biomedical materials 2015; 10:045023; PMID:26290516; http://dx.doi.org/10.1088/1748-6041/10/4/045023

[17] He H, Liu X, Peng L, Gao Z, Ye Y, Su Y, Zhao Q, Wang K, Gong Y, He F. Promotion of hepatic differentiation of bone marrow mesenchymal stem cells on decellularized cell-deposited extracellular matrix. BioMed research international 2013; 2013:406871; PMID:23991414

[18] Barcellos-de-Souza P, Gori V, Bambi F, Chiarugi P. Tumor microenvironment: bone marrow-mesenchymal stem cells as key players. Biochim Biophys Acta 2013; 1836:321-35; PMID:24183942

[19] Hwang S, Hong HN, Kim HS, Park SR, Won YJ, Choi ST, Choi D, Lee SG. Hepatogenic differentiation of mesenchymal stem cells in a rat model of thioacetamide-induced liver cirrhosis. Cell Biol Int 2012; 36:279-88; PMID:21966929; http://dx.doi.org/10.1042/CBI20110325

[20] Li J, Li L. Immediate intraportal transplantation of human bone marrow mesenchymal stem cells prevents death from fulminant hepatic failure in pigs. Hepatology 2012; 56(3):1044-52; PMID:22422600

[21] Peng L, Xie DY, Lin BL, Liu J, Zhu HP, Xie C, Zheng YB, Gao ZL. Autologous bone marrow mesenchymal stem cell transplantation in liver failure patients caused by hepatitis B: short-term and long-term outcomes. Hepatology 2011; 54:820-8; PMID:21608000; http://dx.doi.org/10.1002/hep.24434

[22] Christ B, Dollinger MM. The generation of hepatocytes from mesenchymal stem cells and engraftment into the liver. Curr Opin Organ Transplant 2011; 16:69-75; PMID:21150616; http://dx.doi.org/10.1097/MOT.0b013e3283424f5b

[23] Lee KD, Kuo TK, Whang-Peng J, Chung YF, Lin CT, Chou SH, Chen JR, Chen YP, Lee OK. In vitro hepatic differentiation of human mesenchymal stem cells. Hepatology 2004; 40:1275-84; PMID:15562440; http://dx.doi.org/10.1002/hep.20469

[24] Badylak SF, Weiss DJ, Caplan A, Macchiarini P. Engineered whole organs and complex tissues. Lancet 2012; 379:943-52; PMID:22405797; http://dx.doi.org/10.1016/S0140-6736(12)60073-7

[25] Song JJ, Ott HC. Organ engineering based on decellularized matrix scaffolds. Trends Mol Med 2011; 17:424-32; PMID:21514224; http://dx.doi.org/10.1016/j.molmed.2011.03.005

[26] Mirmalek-Sani S-H, Sullivan DC, Zimmerman C, Shupe TD, Petersen BE. Immunogenicity of Decellularized Porcine Liver for Bioengineered Hepatic Tissue. Am J Pathol 2013; 183(2):558-65; PMID:23747949

[27] Yagi H, Fukumitsu K, Fukuda K, Kitago M, Shinoda M, Obara H, Itano O, Kawachi S, Tanabe M, Coudriet GM, et al. Human-Scale Whole-Organ Bioengineering for Liver Transplantation: a Regenerative Medicine Approach. Cell Transplant 2012; 22(2):231-42

[28] Zhou P, Lessa N, Estrada DC, Severson EB, Lingala S, Zern MA, Nolta JA, Wu J. Decellularized Liver Matrix as a Carrier for the Transplantation of Human Fetal and Primary Hepatocytes in Mice. 2011:418-27

[29] Crapo PM, Gilbert TW, Badylak SF. An overview of tissue and whole organ decellularization processes. Biomaterials 2011; 32:3233-43; PMID:21296410; http://dx.doi.org/10.1016/j.biomaterials.2011.01.057

[30] Gilbert TW. Strategies for tissue and organ decellularization. J Cell Biochem 2012; 113:2217-22; PMID:22415903; http://dx.doi.org/10.1002/jcb.24130

[31] Baptista PM, Siddiqui MM, Lozier G, Rodriguez SR, Atala A, Soker S. The use of whole organ decellularization for the generation of a vascularized liver organoid. Hepatology (Baltimore, Md) 2011; 53:604-17; PMID:21274881; http://dx.doi.org/10.1002/hep.24067

[32] Ren H, Shi X, Tao L, Xiao J, Han B, Zhang Y, Yuan X, Ding Y. Evaluation of two decellularization methods in the development of a whole-organ decellularized rat liver scaffold. Liver Int 2013; 33:504-15; PMID:23279742

[33] Shirakigawa N, Ijima H, Takei T. Decellularized liver as a practical scaffold with a vascular network template for liver tissue engineering. Journal of bioscience and bioengineering 2012; 114:546-51; PMID:22717723; http://dx.doi.org/10.1016/j.jbiosc.2012.05.022

[34] Ji R, Zhang N, You N, Li Q, Liu W, Jiang N, Liu J, Zhang H, Wang D, Tao K, et al. The differentiation of MSCs into functional hepatocyte-like cells in a liver biomatrix scaffold and their transplantation into liver-fibrotic mice. Biomaterials 2012; 33:8995-9008; PMID:22985996; http://dx.doi.org/10.1016/j.biomaterials.2012.08.058

[35] Jiang WC, Cheng YH, Yen MH, Chang Y, Yang VW, Lee OK. Cryo-chemical decellularization of the whole liver for mesenchymal stem cells-based functional hepatic tissue engineering. Biomaterials

2014; 35:3607-17; PMID:24462361; http://dx.doi.org/10.1016/j.biomaterials.2014.01.024

[36] Takebe T, Sekine K, Enomura M, Koike H, Kimura M, Ogaeri T, Zhang R-R, Ueno Y, Zheng Y-W, Koike N, et al. Vascularized and functional human liver from an iPSC-derived organ bud transplant. Nature 2013; 499(7459):481-4; PMID:23823721

[37] Dou K, Wang D, Tao K, Yue S, Ti Z, Song Z, Li L, He Y, Hou X. A modified heterotopic auxiliary living donor liver transplantation: report of a case. Annals of hepatology 2014; 13:399-403; PMID:24756018

[38] Xiang J, Zheng X, Zhu X, Yang L, Gao R, Li J, Liu X, Lv Y. Optimization of the protocols for in vitro culture and induction of hepatic differentiation of rat mesenchymal stem cells. Nan fang yi ke da xue xue bao = Journal of Southern Medical University 2015; 35:1090-6; PMID:26277502